

MULTIPLE IMAGING OF PULSARS BY REFRACTION IN THE INTERSTELLAR MEDIUM

J. M. CORDES¹

Astronomy Department and National Astronomy and Ionosphere Center, Cornell University

AND

A. WOLSZCZAN

National Astronomy and Ionosphere Center, Cornell University

Received 1986 March 10; accepted 1986 April 30

ABSTRACT

We demonstrate, using dynamic spectra of interstellar scintillations, that pulsar images are sometimes multiple and that images change on time scales of days to months. Component separations as large as 4 mas at 430 MHz are twice the scattering diameter of each component which, in turn, is at least 10^4 times the intrinsic source size. We discuss the implications of our results for VLBI, for timing measurements of pulsars, and for the form of the interstellar electron-density wavenumber spectrum.

Subject headings: interstellar: matter — interferometry — pulsars — turbulence

I. INTRODUCTION

All radio signals are scattered, to varying degrees, as they propagate through electron density turbulence in the interstellar medium (ISM). Scattering causes angular broadening of source images and, under certain conditions, intensity scintillations in time and frequency. Recent work (Rickett, Coles, and Bourgois 1984; Blandford and Narayan 1985; Cordes, Pidwerbetsky, and Lovelace 1986) has been concerned with distinguishing *refractive* from *diffractive* scintillations because the former may cause intensity variations from many kinds of radio sources, while the latter is visible only from pulsars, owing to their small size.

In this *Letter*, we report preliminary results from a study of pulsar scintillations at the Arecibo Observatory. We discuss three pulsars which show, at some epochs, dynamic spectra (i.e. intensity as a function of frequency and time) with oscillations and/or multiple drift rates due to a combination of *multipath* refractive scattering and diffractive scattering.

We obtained dynamic spectra in 1980 November, 1981 August, and from 1984 August to 1985 June using a 1 bit autocorrelation spectrometer gated synchronously with the pulsar. ON and OFF pulse spectra of 252 samples each were recorded at ~ 10 s intervals for total observation times ≤ 90 minutes using bandwidths of 1.25 MHz for PSR 0919+06 and 10 MHz for PSR 1133+16 and PSR 1919+21. Details of the data acquisition and analysis are given by Cordes, Weisberg, and Boriakoff (1983, 1985, hereafter CWB 1983 and CWB 1985).

II. ANALYSIS OF DYNAMIC SPECTRA

It is conventional to determine the characteristic time scale Δt_d and frequency scale $\Delta \nu_d$ of the scintillations as the half-widths at half-maxima of a two-dimensional autocovariance function (ACV) of the dynamic spectra (e.g., Cordes

1986). The ACV has units of intensity squared. Systematic “drifts” are characterized by a drift rate, $d\nu/dt$, which is given by the major axis of the ACV. It is usual practice to interpret the time and frequency scales in terms of an implied *diffraction* angle θ_d , due to irregularities $< (\lambda D)^{1/2} \approx 10^{11}$ cm (D is the distance), while the drift rate is a refractive alteration of the diffraction pattern associated with irregularities $> (\lambda D)^{1/2}$, characterized by a *refraction* angle θ_r . For a thin scattering screen at distance D , these quantities are related according to $\Delta t_d \approx \lambda/2\pi\theta_d V_\perp$, $\Delta \nu_d \approx c/\pi D\theta_d^2$, and $d\nu/dt \approx \nu V_\perp/2D\theta_r$, where V_\perp is a transverse speed (Hewish 1980). Were it not for the appearance of oscillations and multiple drift rates in dynamic spectra, these quantities would suffice in characterizing the scintillations. We discuss data that show such oscillations and, in the next section, extend the above model to explain the oscillations.

Figure 1a (Plate L1) shows dynamic spectra from PSR 0919+06 with randomly placed intensity maxima that are consistent with single-image diffractive scattering. This pattern was maintained for the last 5 months of 1984, followed by a 6 month long episode of multiple drift rates and oscillations, after which it reverted to a state of random structure. Figures 1b and 1c show dynamic spectra with strong oscillations and drift. The patterns maintained the same form for a few days but obviously changed over the 2 weeks separating the two epochs.

Previous work has also identified oscillations in dynamic spectra (Roberts and Ables 1982; Hewish, Wolszczan, and Graham 1985; CWB 1985). The oscillations are clearly not instrumental because they appear at only some epochs for a given object and with time-dependent parameters; at a specific epoch, they do not occur for all objects observed; and the oscillations are unlike any associated with reflections off the telescope structure.

Figure 2a (Plate L2) shows spectra for PSR 1133+16 during an episode of strong oscillations. Like 0919+06, this

¹Alfred P. Sloan Foundation Fellow.

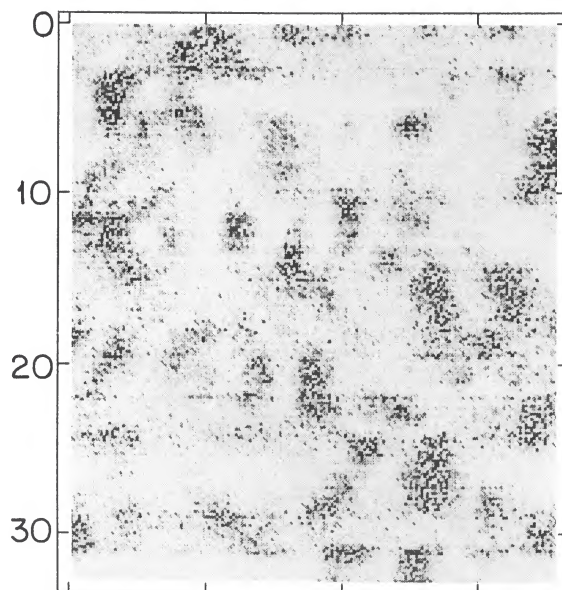


Figure 1a

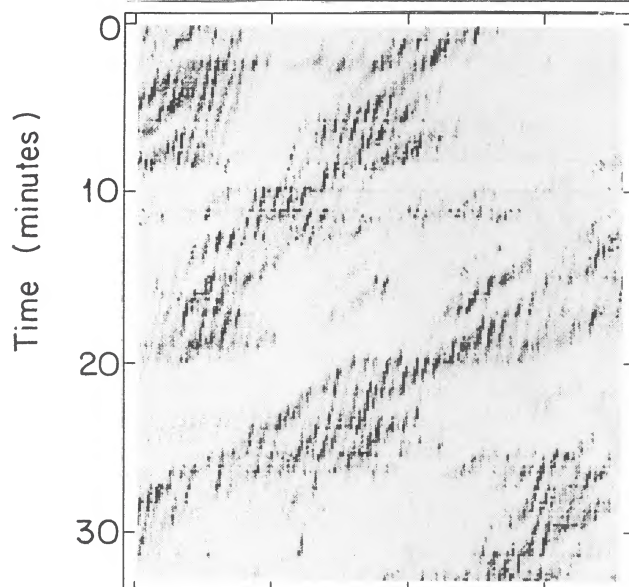


Figure 1b

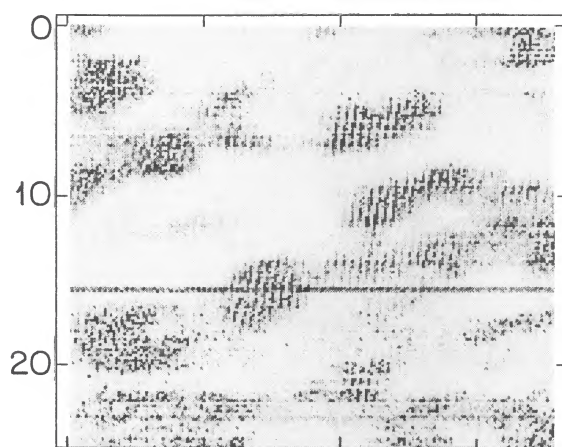


Figure 1c

429.7 430.2
Frequency (MHz)

FIG. 1.—Dynamic spectra of PSR 0919+06 at 430 MHz for three epochs. (a) 1984 August (1984.66); (b) 1985 May (1985.40); (c) 1985 June (1985.44). The horizontal line is due to lightning interference.

CORDES AND WOLSZCZAN (*see* page L27)

PLATE L2

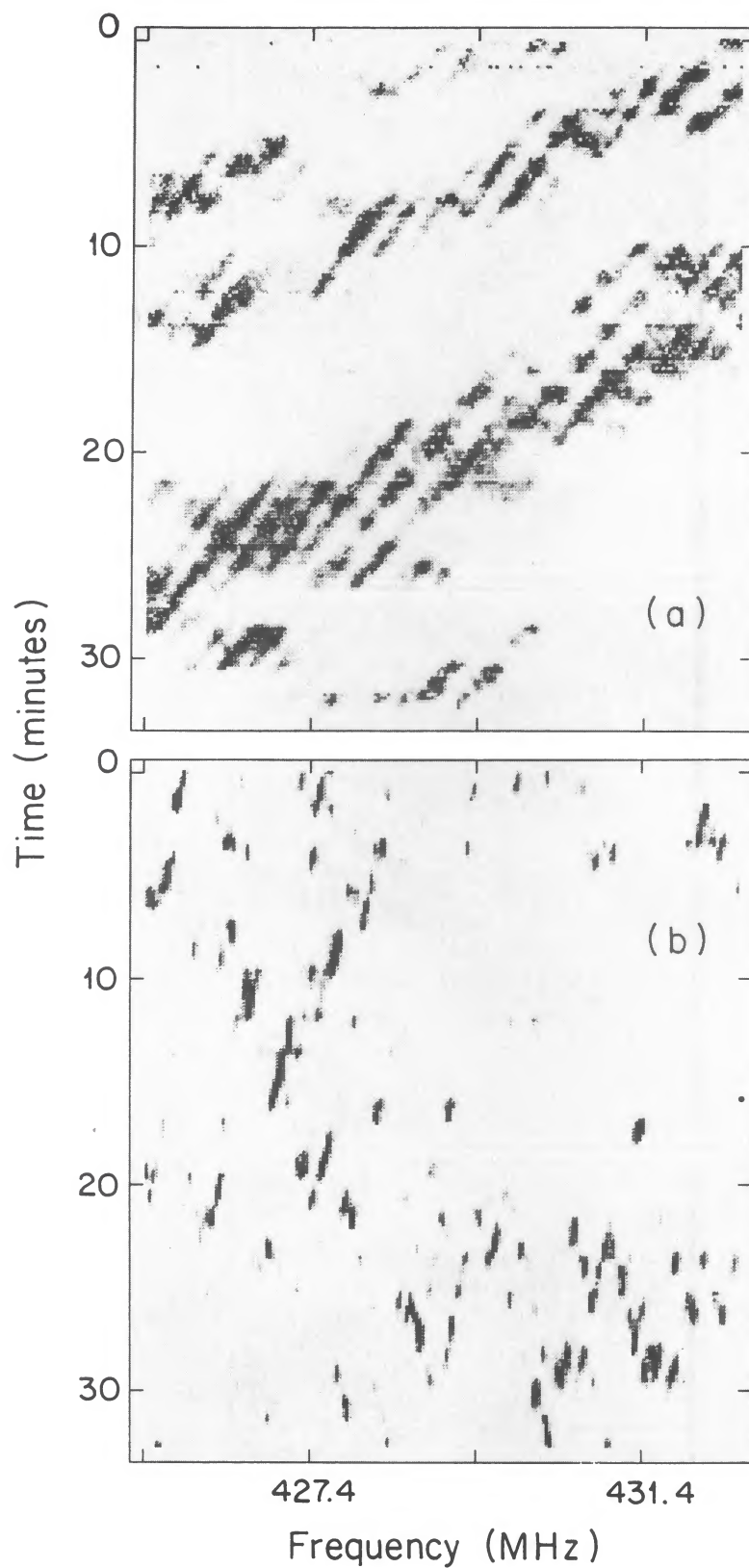


FIG. 2.—Dynamic spectra for two pulsars at 430 MHz. (a) PSR 1133+16 at 1984 November (1984.89); (b) PSR 1919+21 at 1981 August (1981.61). CORDES AND WOLSZCZAN (*see* page L27)

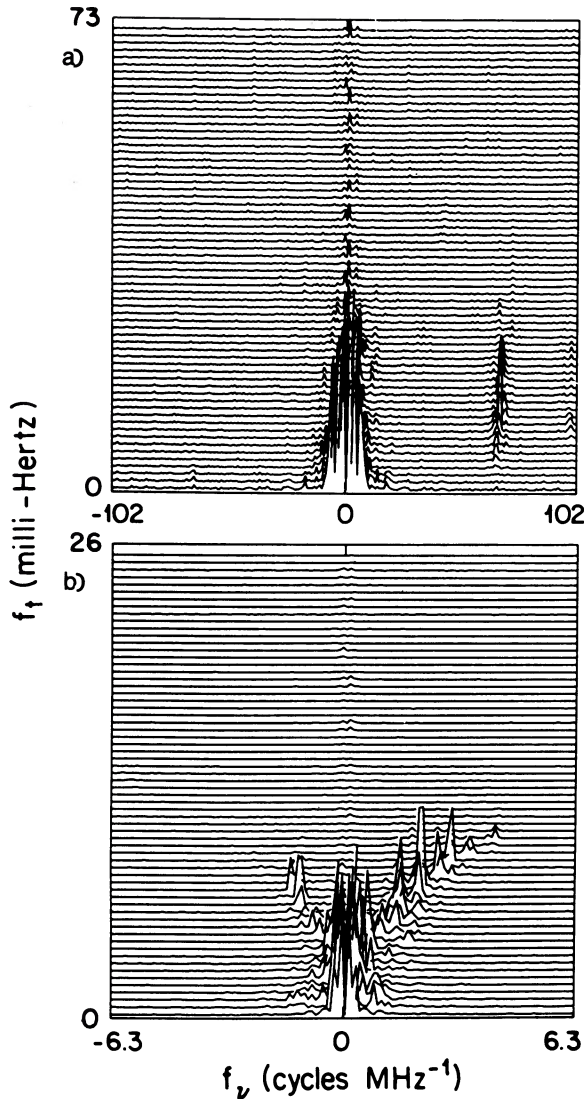


FIG. 3.—Two-dimensional power spectra of dynamic spectra. (a) For data from 0919+06 given in Fig. 1c. The maximum plotted point is 2% of the overall maximum. (b) For data from 1133+16 given in Fig. 2a. The maximum plotted value is 6% of the overall maximum.

pulsar shows, at different epochs, both oscillating and non-oscillating scintillations, but with a smaller time scale for change, probably because it is nearer than 0919+06 and has a larger space velocity. PSR 1919+21 shows oscillations at some epochs, but its scintillations were dominated by a dual drift rate in both 1980 and 1981. Dynamic spectra (Fig. 2b) show obvious drifts in two directions. Dual frequency observations (430 and 320 MHz) show the same dual drift pattern, but with drift rates larger at 430 MHz. The rates do not scale precisely as $d\nu/dt \propto \nu^3$, but we think this is due to our crude estimation of the drift rates.

We calculated two-dimensional fluctuation spectra of the dynamic spectra in order to identify and quantify the oscillations. The coordinates of these spectra are fluctuation frequencies f_ν and f_t that have units of time (cycles per Hz) and frequency (cycles per second), respectively. Such spectra dis-

play a feature near the origin that is produced by diffractive scintillations. A ridge along the f_t axis is due to intrinsic, broad-band intensity variations. Other features correspond to periodicities in the dynamic spectra.

The two-dimensional fluctuation spectrum in Figure 3a for the dynamic spectra of Figure 1c reveals a well-defined component at $f_\nu \approx 71 \mu s$ and $f_t \approx 14$ MHz with an amplitude $\sim 10\%$ of the feature at zero frequency. The data in Figure 1b have a power spectrum (not shown) with two predominant features, implying two distinct periodicities. The fluctuation spectrum for 1133+16 (Fig. 3b) shows many components other than the one near the origin.

The Fourier transform of the fluctuation spectrum is the ACV. The ACV for 1919+21 (Fig. 4) displays two ridges whose slopes yield drift rates, $d\nu/dt$. Also shown are cuts along the two axes. The widths of these cuts are the scintillation scales $\Delta\nu_d$ and Δt_d .

Table 1 gives values for diffraction bandwidths, time scales, drift rates, and oscillation periods for the three objects.

III. MULTIPLE IMAGES

To account for oscillations in dynamic spectra, consider a thin screen which scatters an incoming plane wave into two smeared-out images, each of size θ_d , at angles θ_1 and θ_2 with respect to a direct ray from the screen to the observer. If $|\theta_2 - \theta_1| > 2\theta_d$, each image yields an independent diffraction pattern. The two diffraction patterns superpose with an interference term that results because the screen is illuminated with a coherent radiation field.

In reality, the screen model is not justified because scattering seems to occur through a large fraction of the line of sight (CWB 1985). For an extended medium, oscillation periods are related to *path-length differences* between rays reaching the observer, but these are *not* related to the *observed* angular separations of the rays. In this case, the true image cannot be reconstructed but oscillations can be used to estimate *statistical properties*, such as the frequency of occurrence of multiple images and typical angular separations.

Letting $I_{1,2}(\nu, t)$ be the dynamic spectra that would be produced by each image alone, we write the net dynamic spectrum in the form

$$I(\nu, t) = I_1(\nu, t) + I_2(\nu, t) + 2[I_1(\nu, t)I_2(\nu, t)]^{1/2} \times \cos[\Phi(\nu, t) + \phi(\nu, t)]. \quad (1)$$

The phase $\Phi \approx \pi D \lambda^{-1}(\theta_2^2 - \theta_1^2)$ is the geometrical difference in path lengths between the observer and the two points on the phase screen while ϕ is a random phase due to irregular structure in the screen. The sinusoidal cross term, which has oscillation periods P_ν and P_t , is *amplitude-modulated* by $(I_1 I_2)^{1/2}$ and *phase-modulated* by ϕ . The fluctuating part of $I(\nu, t)$ would be dominated by the cosine term if diffraction were negligible. Such highly organized dynamic spectra are generally not seen. For N images, the dynamic spectrum is the sum of N independent dynamic spectra and $N(N-1)/2$ cross terms.

The random phase ϕ varies with characteristic time and frequency scales Δt_d and $\Delta\nu_d$. The geometrical phase Φ ,

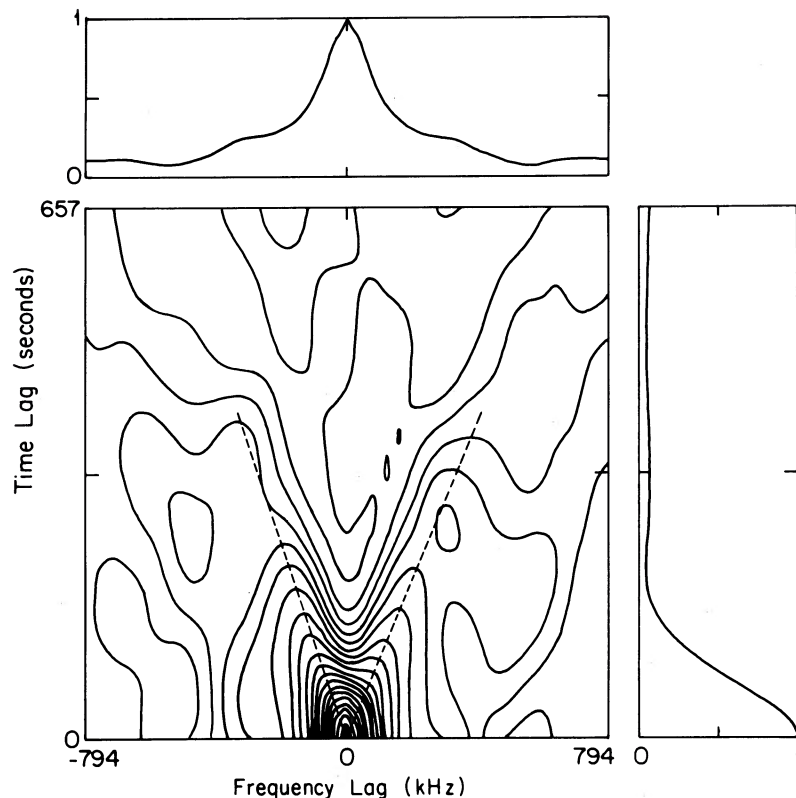


FIG. 4.—Two-dimensional intensity autocovariance function for PSR 1919+21 at 430 MHz. The straight dashed lines show the dual drift rates. Contours are from 0 to 1 at intervals of 0.05. Also shown are slices along the coordinate axes.

TABLE 1
SCINTILLATION PARAMETERS

Epoch (1)	ν (GHz) (2)	$\Delta\nu_d^a$ (kHz) (3)	Δt_d^a (s) (4)	$\frac{d\nu^a}{dt}$ (kHz s ⁻¹) (5)	P_ν^a (kHz) (6)	P_t^a (s) (7)	θ_d (mas) (8)	θ_r (mas) (9)	θ_{split} (mas) (10)
0919+06									
1984.66.....	0.43	34	90	0.05	3.3	3.4	...
1985.40.....	0.43	90	126	-0.43	21	232	2.0	-0.4	3.6
1985.44.....	0.43	61	87	-0.36	115	150	1.5
1985.44.....	0.43	61	87	-0.36	14	72	2.4	-0.5	4.4
1133+16 ^b									
1984.89.....	0.43	850	80	-6.9	360	110	1.6	-0.17	2.2
...	480	133	1.9
...	710	170	1.5
...	-710	141	1.5
1919+21									
1981.60.....	0.43	103	79	1.03	320	330	3.1	0.25	1.5
...	-0.82	-0.32	...
1981.61.....	0.32	55	72	0.57	140	380	4.3	0.34	2.3
...	-0.45	-0.43	...

^aErrors in the scintillation quantities in cols. (3)–(7) are $\pm 10\%$.

^bThe periodicities identified for 1133+16 are only the most obvious ones; more can clearly be seen in Fig. 3.

which may vary on much larger scales, can be expanded as $\Phi(\nu + \delta\nu, t + \delta t) \approx \Phi(\nu, t) + 2\pi(\delta\nu/P_\nu + \delta t/P_t)$, where $\Phi \approx 10^{3.9} \nu_{\text{GHz}} D_{\text{kpc}} (\theta_2^2 - \theta_1^2)$ radians, $P_\nu \approx 0.27 D_{\text{kpc}}^{-1} (\theta_2^2 - \theta_1^2)^{-1}$ MHz, and $P_t \approx 10^{2.8} [\nu_{\text{GHz}} V_{100} (\theta_2 - \theta_1)]^{-1}$ s. Here angles are in units of milliarcsec (mas) and V_{100} is the transverse speed in units of 100 km s^{-1} .

The model can account for the data that we have presented. For PSR 0919+06, the fringes in Figure 1c undergo a phase shift between one diffractive maximum and another, as is predicted by the model. For both 0919+06 and 1133+16, the fringes are produced by more than two images, because there are several features in the two-dimensional fluctuation spectrum. For 1919+21 the dual drifts suggest that two sub-images dominate the brightness distribution. A periodicity is also evident in the fluctuation spectrum (not shown).

In Table 1 we give values of θ_d , θ_r , and $\theta_{\text{split}} \equiv (\theta_2^2 - \theta_1^2)^{1/2}$ using expressions given above. We have also assumed distances of 1, 0.16, and 0.36 kpc and transverse speeds of 117, 130, and 65 km s^{-1} for 0919+06, 1133+16, and 1919+21, respectively. The distances are from Manchester and Taylor (1981), and the speeds are scintillation derived (Cordes 1986).

IV. DISCUSSION

We have shown that refractive scattering produces multiple images of three pulsars at some epochs. In fact, most of the ~ 30 pulsars we have studied at Arecibo show similar effects (oscillations and multiple drift rates in dynamic spectra) some of the time. Therefore, multipath refractive scattering must be a common occurrence, a fact that has implications for the power spectrum of electron-density variations in the ISM, for VLBI of scattered sources, and timing measurements of pulsars.

The electron density power spectrum is thought to be of the form (wavenumber) $^{-\alpha}$ over several decades of wavenumber corresponding to scales near $\sim 10^{11}$ cm. The exponent α is often estimated to be less than 4 and near the "Kolmogorov" value of $11/3$ from dynamic spectra of pulsars (Rickett 1977; Armstrong, Cordes, and Rickett 1981; Wolszczan 1983; CWB 1985; Smith and Wright 1985). However, recent studies of "refractive" intensity variations alternatively suggest values slightly in excess of 4 (Hewish, Wolszczan, and Graham 1985; Romani, Blandford, and Narayan 1985). In strong scattering, a "shallow" spectrum like the Kolmogorov spectrum is not expected to produce multiple images. This follows because refraction angles from such media are much smaller than the diffractive smearing, $\theta_r/\theta_d \ll 1$ (unless the inner scale $\approx (\lambda D)^{1/2}$, and the spectrum amplitude is correspondingly larger). Steeper power laws yield considerably more refraction, so $\theta_r/\theta_d \gg 1$, and the probability of obtaining multiple images is larger (Lovell 1970; Cordes, Pidwerbetsky, and Lovell 1986).

We conclude that at least *some* portion of the actual electron-density spectrum must have an effective $\alpha > 4$ for *some* lines of sight through the ISM. However, since we find compelling other studies (Armstrong and Rickett 1980; Wolszczan 1983) which suggest conformance at "large" wavenumbers to an $\alpha < 4$ spectrum, we propose that the actual spectrum may be a "hybrid" spectrum that is Kolmogorov-like at large wavenumbers but steeper at low wavenumbers.

Images of scattered radio sources derived from VLBI will be strongly affected at frequencies where scattering is strong ($\nu \leq 5$ GHz). One may expect to see asymmetric images that change on a refractive time scale. Although this time scale is short for pulsars discussed in this *Letter*, it could be very long for objects such as the compact source in the Galactic center, Sgr A, for which an asymmetry has been seen (Lo *et al.* 1985).

Time of arrival fluctuations $\delta t \approx D\theta_r^2/2c \approx 1.2 \mu\text{s} D_{\text{kpc}} \theta_r^2$ (θ_r in units of mas) are expected on time scales of weeks to months. These are geometric in origin, scale as λ^4 , and are different from the dispersive variations $\propto \lambda^2$ considered by Armstrong (1984). The amplitude and time scale are strongly pulsar dependent because the amplitude of the wavenumber spectrum varies strongly between different lines of sight (CWB 1985). Moreover, the extrapolation to longer time scales is uncertain because it depends on the low-wavenumber portion of the spectrum, which is poorly constrained. During episodes of multiple imaging, the pulsar pulse is multiple with time separations of the same order as δt calculated above. It may be possible to detect such separations for the millisecond pulsar 1937+214, whose pulse width is narrow ($\sim 40 \mu\text{s}$; Cordes and Stinebring 1984).

The oscillations in dynamic spectra are analogous to fringes from an *effective* interferometer with baseline ~ 1 AU. By comparing dynamic spectra obtained for different pulse components of a pulsar (e.g., looking for a phase shift in oscillations such as those in Fig. 1c), one may be able to resolve pulsar magnetospheres at angular scales < 1 micro-arcsec (Cordes, Pidwerbetsky, and Lovell 1986). This method has better resolution than the purely diffractive approach of CWB (1983) if $P_\nu \ll \Delta\nu_d$.

We thank J. Armstrong, W. Coles, T. Gold, T. Hagfors, R. Lovell, R. Narayan, A. Pidwerbetsky, and B. Rickett for helpful discussions; R. Dewey, A. Pidwerbetsky, and L. Feinswog for help in the data analysis; and J. Weisberg and V. Boriakoff for help in obtaining the data in 1980 and 1981. This research was supported by an Alfred P. Sloan Foundation Fellowship, by NSF grant AST 8311844, and by the National Astronomy and Ionosphere Center, which is operated by Cornell University under contract with the NSF.

REFERENCES

- Armstrong, J. W. 1984, *Nature*, **307**, 527.
 Armstrong, J. W., and Rickett, B. J. 1980, *M.N.R.A.S.*, **194**, 623.
 Armstrong, J. W., Cordes, J. M., and Rickett, B. J. 1981, *Nature*, **291**, 561.
 Blandford, R., and Narayan, R. 1985, *M.N.R.A.S.*, **213**, 591.
 Cordes, J. M. 1986, *Ap. J.*, in press.
 Cordes, J. M., Pidwerbetsky, and Lovell, R. V. E. 1986, *Ap. J.*, in press.
 Cordes, J. M., and Stinebring, D. 1984, *Ap. J. (Letters)*, **277**, L53.
 Cordes, J. M., Weisberg, J. M., and Boriakoff, V. 1983, *Ap. J.*, **268**, 370 (CWB 1983).
 ———. 1985, *Ap. J.*, **288**, 221 (CWB 1985).

- Hewish, A. 1980, *M.N.R.A.S.*, **192**, 799.
Hewish, A., Wolszczan, A., and Graham, D. 1985, *M.N.R.A.S.*, **213**, 167.
Lo, K. Y., Backer, D. C., Ekers, R. D., Kellerman, K. I., Reid, M. J., and Moran, J. M. 1985, *Nature*, **319**, 124.
Lovell, R. V. E. 1970, Ph.D. thesis, Cornell University.
Manchester, R. N., and Taylor, J. H. 1981, *A.J.*, **86**, 1953.
Rickett, B. J. 1977, *Ann. Rev. Astr. Ap.*, **15**, 479.
Rickett, B. J., Coles, W. A., and Bourgois, G. 1984, *Astr. Ap.*, **134**, 390.
Roberts, J. A., and Ables, J. G. 1982, *M.N.R.A.S.*, **201**, 1119.
Romani, R. W., Narayan, R., and Blandford, R. 1985, preprint.
Smith, F. G., and Wright, N. C. 1985, *M.N.R.A.S.*, **214**, 97.
Wolszczan, A. 1983, *M.N.R.A.S.*, **204**, 591.

J. M. CORDES: Center for Radiophysics and Space Research, Cornell University, Space Sciences Building, Ithaca, NY 14853-0355

A. WOLSZCZAN: Arecibo Observatory, P.O. Box 995, Arecibo, PR 00613